

^(a)Work performed while a visitor at Argonne National Laboratory, Argonne, Ill. 60439.

¹H. A. Thiessen *et al.*, to be published, and LASL Report No. LA-4534 MS, 1970 (unpublished).

²E. Borie, *Phys. Lett.* **68B**, 433 (1977).

³K. Boyer *et al.* to be published.

⁴P. J. Bussey, J. R. Carter, D. R. Dance, D. V. Bugg, A. A. Carter, and A. M. Smith, *Nucl. Phys.* **B58**, 363 (1973).

⁵J. Piffaretti, R. Corfu, J. P. Egger, P. Gretillat, C. Lunke, E. Schwarz, C. Perrin, and B. M. Preedom, *Phys. Lett.* **71B**, 324 (1977).

⁶R. A. Eisenstein and F. Tabakin, *Comput. Phys. Commun.* **12**, 237 (1976).

⁷D. H. Herndon, A. Barbaro-Galtieri, and A. H. Ro-

senfeld, Lawrence Radiation Laboratory Report No. UCRL-20030 πN , 1970 (unpublished).

⁸J. Londergan, R. McVoy, and E. Moniz, *Ann. Phys.* (N.Y.) **86**, 147 (1974).

⁹C. W. DeJager, H. DeVries, and C. DeVries, *At. Data Nucl. Data Tables* **14**, 479 (1974).

¹⁰E. T. Boschitz, in *Proceedings of the International Conference on High-Energy Physics and Nuclear Structure, Zurich, 1977*, edited by M. P. Locher (Birkhauser-Verlag, Basel, Switzerland), p. 133, and private communication.

¹¹E.g., J. A. Nolen and J. P. Schiffer, *Annu. Rev. Nucl. Sci.* **10**, 471 (1969); S. Shlomo and E. Friedman, *Phys. Rev. Lett.* **39**, 1180 (1977), and references therein.

Precision Laser Photodetachment Spectroscopy in Magnetic Fields

W. A. M. Blumberg, R. M. Jopson, and D. J. Larson

Lyman Laboratory of Physics, Harvard University, Cambridge, Massachusetts 02138

(Received 15 March 1978)

Magnetic-field-dependent structure in the photodetachment cross section of negative sulfur ions has been observed. This is the first observation of such structure for any negative ion. The structure is found to be due in part to the excitation of the detached electrons to discrete cyclotron levels.

We have observed the effect of a strong magnetic field on the photodetachment cross section of the negative sulfur ion near the threshold for detachment from the $^2P_{3/2}$ state. Part of the motivation for this investigation is the possibility that state-dependent photodetachment might provide an effective method of producing and detecting population differences in certain stored ionic species. S^- was selected for study because at zero magnetic field the photodetachment cross section near threshold is known to be a steeply rising monotonic function of light frequency.¹ We observed that the application of a magnetic field produces structure in the cross section which has a periodic dependence on the light frequency. This structure constitutes a dramatic departure from the behavior at zero magnetic field.^{1,2} We find that the oscillatory structure is due to the excitation of the detached electron to discrete cyclotron (Landau) levels in the magnetic field.³

The only bound states of the group-VI series of atomic negative ions are 2P fine-structure doublet formed from a p^5 configuration. The energy level diagram for S^- as measured by Lineberger and Woodward¹ is shown in Fig. 1. The dependence of the zero-field photodetachment cross section on photon energy was more clearly demonstrated

in experiments on Se^- . Hotop, Patterson, and Lineberger² found that $\sigma \propto (\nu - \nu_{\text{threshold}})^{1/2}$, thus verifying the Wigner prediction⁴ for experimental resolution on the order of 2 cm^{-1} and for energies of less than 40 cm^{-1} above threshold. The measurements reported in this paper involve at

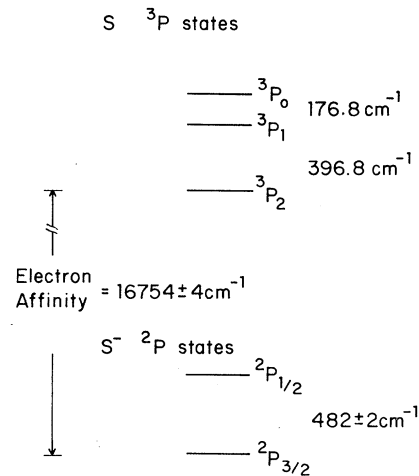


FIG. 1. Zero-field energy levels of S^- and S. The $^2P_{3/2} \rightarrow ^3P_2$ transition has been used for all of the results reported in this paper.

most a photon energy of 4 cm^{-1} above threshold with a Doppler-limited resolution of about 0.1 cm^{-1} .

The Wigner prediction can be simply understood in terms of the golden rule. The bound p electron in the negative ion can be promoted to a continuum s or d state. Sufficiently near threshold, the d state is highly suppressed by the angular-momentum barrier. The matrix element for a transition to the s state is independent of the energy in the final state to first order since the s wave electron penetrates to the neutral atom even at zero kinetic energy. The density of final states is proportional to k (where k is the relative momentum of e^- and S^-). Thus, the total transition probability near threshold is proportional to k which is nearly equal to the final electron momentum. In the presence of a magnetic field, the transverse motion of the detached electron is constrained, leaving only one degree of freedom. The density of final states then becomes proportional to $1/k_z$ (where z is the coordinate along the direction of the field) rather than proportional to k .⁵ This dependence upon k_z also holds for the cross section in the low-field limit since the transition matrix element is not substantially altered and remains independent of k_z to first order. The effect of the magnetic field is thus to change the cross section from one which has an infinite slope at threshold and rises monotonically to one which in first approximation is infinite at threshold and falls rapidly above the threshold.⁶

The central piece of experimental apparatus is an ion trap in which a gas of S^- ions is created, depleted by photodetachment, and detected. The trap is of the Penning design⁷ and consists of three copper electrodes: two end caps and a ring. The surfaces of the electrodes are conjugate truncated hyperboloids of revolution which produce an electrostatic potential approximately of the form, $\varphi = V(r^2 - 2z^2)/4z_0^2$ when a voltage V is applied between the ring and the end caps. The distance, z_0 , from the center of the trap to each end cap is 0.100 in. An axial magnetic field on the order of 10 kG confines the ions radially. Three independent harmonic motions occur in this combination of electric and magnetic fields. There is an axial oscillation of frequency ν_z and two transverse modes: a cyclotron oscillation of frequency ν_c' and a magnetron precession of frequency ν_m where, $\nu_c' \nu_m = \nu_z^2/2$. For a field of 10 kG and an applied potential of 1.35 V, S^- ions oscillate at the frequencies, $\nu_z = 125 \text{ kHz}$, $\nu_c' = 459 \text{ kHz}$, and

$\nu_m = 17 \text{ kHz}$. We have observed lifetimes of many minutes for positive ions under similar conditions with a background gas pressure of about 10^{-9} Torr.

Ions are created in the trap by the dissociative attachment process, $e^- + \text{OCS} \rightarrow \text{CO} + S^-$, that occurs with a large cross section ($\sigma \approx 3 \times 10^{-17} \text{ cm}^2$) for low-electron energy (1.4 eV).⁸ On the order of 10^4 ions are created during each data cycle by a 10^{-7} -A beam of electrons incident on OCS leaked into the trap at a few times 10^{-8} Torr. The electrons are injected axially through a hole in one end cap. The S^- lifetime is limited to a few seconds due to reaction with the OCS background. The dominant reaction appears to be $S^- + \text{OCS} \rightarrow \text{CO} + S_2^-$.

Light of approximately 597-nm wavelength is provided by a cw dye laser which emits over 100 mW with a bandwidth of less than 10 MHz. The wavelength was selected to probe the $^2P_{3/2} \rightarrow ^3P_2$ threshold in the S^- ions. The amount of light sent through the trap in each data cycle is monitored and the integrated intensity is held constant from cycle to cycle. Figure 2(a) shows some elements of the optical system.

The number of ions is detected by driving them

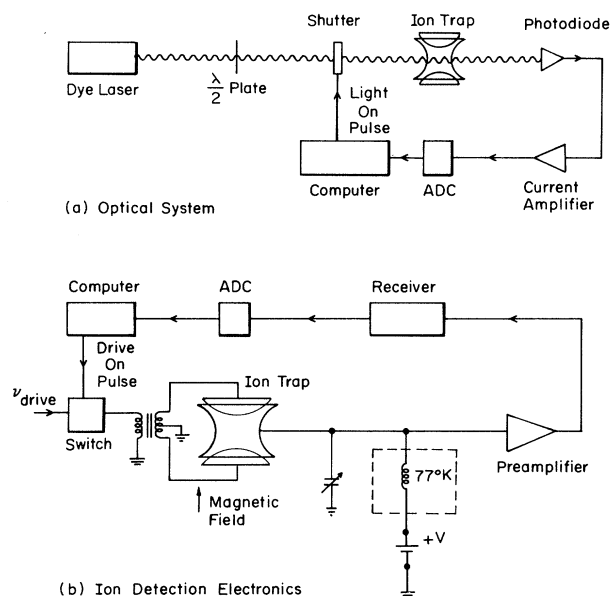


FIG. 2. Schematic diagrams of the experimental apparatus. The ions undergo photodetachment with light of a selected polarization and constant integrated intensity as illustrated in (a) and those remaining are detected (b) by driving at their axial resonant frequency and measuring the current induced on the ring electrode.

at their axial frequency ν_z , with an rf voltage applied across the end caps. The image current at frequency $2\nu_z$ flowing between the ring and ground is detected in a tuned circuit which is cooled to 77°K to reduce thermal noise. The voltage across the tuned circuit is amplified, mixed down to 5 kHz and detected in a bandwidth of 200 Hz. The rectified voltage is sampled by an analog-to-digital converter and digitally integrated. Figure 2(b) depicts the detection electronics. The detection scheme provides sufficient sensitivity so that the noise (on the order of a percent) on the full ion signal is largely due to the cycle-to-cycle fluctuations in ion number.

A typical data cycle consists of the following sequence. Ions are created for 6 sec. During part of the next 500 ms the ions undergo photodetachment. Then the number of ions surviving is measured by driving the axial motion for 350 ms. The fraction of ions in the $^2P_{3/2}$ state surviving illumination is $F(\nu) = \sum f_i \exp[-A\sigma_i(\nu)]$, where f_i is the initial fractional population of the state m_j

$= i (\sum f_i = 1)$, A is proportional to the integrated light intensity, and $\sigma_i(\nu)$ is the total cross section for photodetachment from the state $m_j = i$ at frequency ν . In the analysis of the data we assume that $F(\nu) = N(\nu)/N(\nu')$ where $N(\nu)$ is the total number of ions surviving illumination with frequency ν and ν' is a frequency below the threshold for detachment from the $^2P_{3/2}$ state. At the light intensities and frequencies used, detachment from the $^2P_{1/2}$ state is essentially complete.

Photodetachment measurements were made at magnetic fields ranging from 6 to 15.7 kG, for light polarized parallel or perpendicular to the magnetic field, and for various amounts of detachment. Figure 3 presents observations at 15.7 kG for π polarization and Fig. 4 presents observations at 10.7 kG for σ polarization. The amount of detachment has been chosen to provide obvious structure. In each case, the data are shown together with a predicted curve which has three variable parameters adjusted to give reasonable agreement with the data. These parameters are the frequency of the first threshold, an overall cross section scale factor, and the average velocity of the ions. The average velocity ($\sim 3 \times 10^5$ cm/sec) obtained in this fashion is about a factor of 2 larger than that obtained from an independent estimate of ion temperature.

As suggested previously, the basic element of the prediction is the assumption that the detached electrons are excited to discrete cyclotron levels

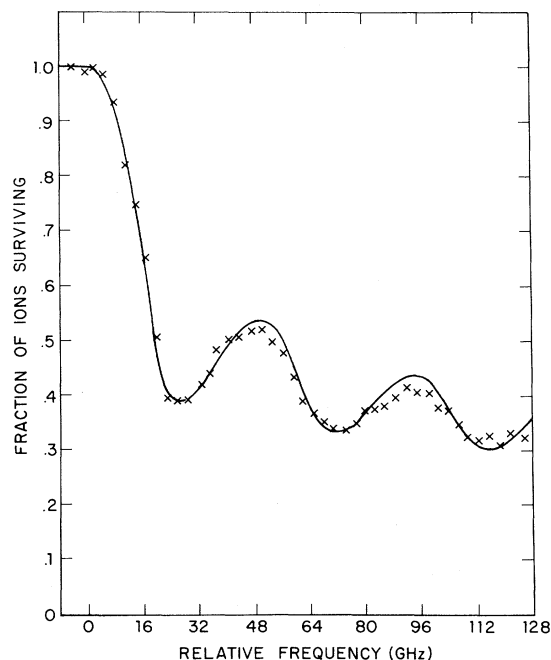


FIG. 3. Photodetachment data near the $^2P_{3/2} \rightarrow ^3P_2$ threshold. The fraction of ions surviving illumination is plotted as a function of light frequency (with an arbitrary zero). The data shown here are for light of π polarization at 15.7 kG. The data points are plotted together with a predicted curve which has three parameters adjusted to give reasonable agreement with the data. The fluctuation in ion number at each point is approximately represented by the size of the point.

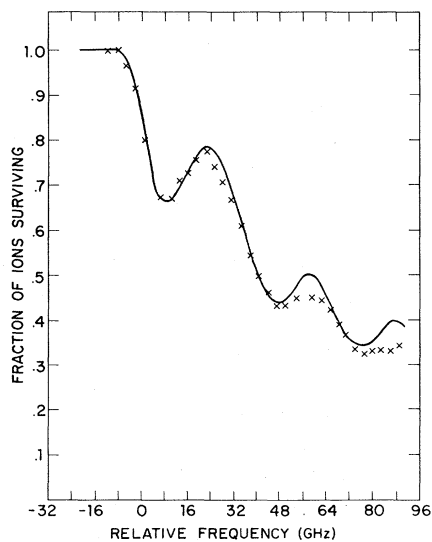


FIG. 4. Photodetachment data as described in Fig. 3 except that the data shown here are for light of σ polarization at 10.7 kG.

and that the cross section for such a transition is proportional to $1/k_z$. Our experimental resolution prevents the observation of discrete Doppler sidebands arising from the harmonic motion of the ions and so the cross section is simply averaged over a Maxwell-Boltzmann velocity distribution. In addition we must take into account the Zeeman structure of the negative ion, neutral atom, and detached electron. This structure, together with the multiplicity of cyclotron levels available to the electron leads to a series of magnetic-field-dependent thresholds. Despite the lack of spherical symmetry in the final state, each transition is weighted by the standard angular momentum coupling coefficients⁹ appropriate for s -wave electrons since for small enough electron momentum and for low enough magnetic fields the wave function of the detached electron appears spherically symmetric in the region near the sulfur atom.

The broad features in the data are due to the excitation of the detached electron to the $m=0$, $n_\rho = 0, 1, 2, \dots$ cyclotron states (where m is the azimuthal component of the electron's orbital angular momentum and n_ρ is the radial quantum number).¹⁰ Each feature consists of a collection of unresolved transitions. The qualitatively different shapes of the curves for σ and π transitions are a result of the different available thresholds and weights for the two cases. The appropriateness of the angular momentum weighing factors is clearly demonstrated by the case of σ polarization where the overlapping of the partial cross sections would wash out the second bump if all transitions were given equal weight. The onset of the π -transition manifold occurs at higher frequency than the onset of the σ -transition manifold. The model predicts a shift of 22 GHz at a magnetic field of 10.7 kG. The observed shift is 20.0 ± 1.4 GHz. This shift is obtained by fitting the cross section near threshold to the predicted cross section.

The dependence of the features on light frequency scales in proportion to the magnetic field. However, it appears that for larger n_ρ 's at a given field and for smaller fields at a given n_ρ the

bumps are smaller than the model predicts. This could possibly be due to collisional effects but the features are observed to be relatively insensitive to OCS background pressure or to the total ion number.

Our results can be summarized by stating that we have observed for the first time magnetic-field-dependent structure in a photodetachment cross section. A basic element of the explanation of this structure is the assumption that the electrons are detached to individual cyclotron levels in the magnetic field. Our model predicts the structure rather well for high fields (~ 15 kG) and small n_ρ (~ 1).

The authors would like to thank W. M. Itano for first suggesting that the cross section in the presence of the magnetic field should be proportional to $1/k_z$. This work was supported by the U. S. Office of Naval Research and the National Science Foundation.

¹W. C. Lineberger and B. W. Woodward, *Phys. Rev. Lett.* **25**, 424 (1970).

²H. Hotop, T. A. Patterson, and W. C. Lineberger, *Phys. Rev. A* **8**, 762 (1973).

³Structure on the optical absorption coefficient in semiconductors with some similarities to our measurements has been observed a number of years ago. See Laura M. Roth, Benjamin Lax, and Solomon Zwerdling, *Phys. Rev.* **114**, 90 (1959).

⁴E. P. Wigner, *Phys. Rev.* **73**, 1002 (1948).

⁵R. H. Garstang, *Rep. Prog. Phys.* **40**, 105 (1977).

⁶W. A. M. Blumberg, W. M. Itano, and D. J. Larson, to be published.

⁷H. Dehmelt, in *Advances in Atomic and Molecular Physics*, edited by D. R. Bates and I. Estermann (Academic, New York, 1967, 1969), Vols. 3 and 5.

⁸J. P. Ziesel and G. J. Schultz, *J. Chem. Phys.* **62**, 1936 (1975).

⁹A. R. P. Rau, in *Electron and Photon Interactions with Atoms*, edited by H. K. Kleinpoppen and M. R. C. McDowell (Plenum, New York, 1976), p. 141; A. R. P. Rau and U. Fano, *Phys. Rev. A* **4**, 1751 (1971).

¹⁰L. D. Landau and E. M. Lifshitz, *Quantum Mechanics: Non-Relativistic Theory* (Addison-Wesley, Reading, Mass, 1965), 2nd ed., p. 424.